water

MDPI

Article

Biogas Production from Palm Oil Mill Effluent Using Dielectric Barrier Discharge Integrated with the Aerated Condition

Reni Desmiarti [1], Maulana Yusup Rosadi [2], Ariadi Hazmi [3,*], Muhammad Miftahur Rahman [4], Nofri Naldi [5] and Joni Aldilla Fajri [6]

[1] Department of Chemical Engineering, Universitas Bung Hatta, Padang 25147, Indonesia
[2] River Basin Research Center, Gifu University, Gifu 501-1193, Japan
[3] Department of Electrical Engineering, Andalas University, Padang 25166, Indonesia
[4] Department of Chemical Engineering, Gajah Mada University, Yogyakarta 55281, Indonesia
[5] Department of Chemistry, Andalas University, Padang 25166, Indonesia
[6] Department of Environmental Engineering, Universitas Islam Indonesia, Yogyakarta 55584, Indonesia
* Correspondence: ariadi@eng.unand.ac.id; Tel.: +62-813-8586-9452

Abstract: In this study, the performance of dielectric barrier discharge (DBD) with the aerated condition at discharge voltages of 15, 20, and 25 kV on the production of biogas; CH_4, H_2, CO, and CO_2 and the removal of COD and BOD from POME were investigated. The experimental results showed that the aerated condition with a rate of 2.5 L/min at a high voltage (25 kV) produced CH_4, CO, and CO_2 that was 9.4, 21.5, and 19.6 times higher than the non-aerated one, respectively. The maximum cumulative volume of CH_4, H_2, CO, and CO_2 was 95.4 ± 8.92, 0.94 ± 0.71, 3.06 ± 0.73, and 2.45 ± 0.35 mL/mg COD, respectively, under the aerated condition at 25 kV and the experimental data fit well with the polynomial regression ($R^2 > 95$) for the initial biogas production. The decrease in COD and BOD was greatly affected by the high discharge voltage under the aerated condition, resulting in a high removal rate. These findings suggest that good performance was observed when the DBD was integrated with the aerated condition under the optimum discharge voltage. The study can give information on the optimum condition in a laboratory scale to produce CH_4, H_2, CO, and CO_2, as well as the reduction of organic pollutants from POME.

Keywords: aerated; non-aerated; biogas; dielectric barrier discharge; palm oil mill effluent

Citation: Desmiarti, R.; Rosadi, M.Y.; Hazmi, A.; Rahman, M.M.; Naldi, N.; Fajri, J.A. Biogas Production from Palm Oil Mill Effluent Using Dielectric Barrier Discharge Integrated with the Aerated Condition. *Water* **2022**, *14*, 3774. https://doi.org/10.3390/w14223774

Academic Editors: Changseok Han, Daphne Hermosilla Redondo, Yeojoon Yoon and Alicia L. Garcia-Costa

Received: 10 September 2022
Accepted: 8 November 2022
Published: 20 November 2022

1. Introduction

Indonesia contributes to 54% of world palm oil production and has become the world's top producer and exporter of palm oil, with production accounting for around 48.4 million metric tons [1,2]. The rapid growth of the palm oil industry to comply with the oil production demand contributes to the large amount of waste generated from the palm oil industry. One of the biggest concerns regarding waste generated from the palm oil industry is high-strength wastewater, known as palm oil mill effluent (POME). POME is generated from the extraction process during palm oil production with an approximate amount of 2600 m^3/ton of crude palm oil [3]. POME is responsible for water pollution when released into the river due to the high biological oxygen demand (BOD), chemical oxygen demand (COD), and complex organic matter such as tannins, lignins, and long-chain fatty acids that are difficult to biodegrade and harmful to the environment [4,5]. POME also contain readily biodegradable matter such as carbohydrates, lipids, and proteins [4,6].

Increasing industrialization has resulted in the rapid expansion of the palm oil industry and led to global environmental pollution awareness due to the generation of POME. The industry is obliged to treat its waste effluent prior to discharging it into streams and rivers. Many POME treatments have been purposed to reduce BOD and COD to comply with the discharge standards for BOD and COD enacted in the Ministry of Environment and Forestry of the Republic of Indonesia (100 and 350 mg/L, respectively). Recent studies have

shown that an electrocoagulation (EC) system is an excellent alternative to POME [7,8]. EC could reduce turbidity, increase the pH value close to neutral, and greatly reduce COD and BOD levels [7,9]. However, the addition of chemicals used for EC might increase the content of hydroxyl metal in POME. Membrane technology has been used widely in industrial wastewater treatment [10,11]. The membrane separation treatment was reported to greatly reduce turbidity, COD, and BOD by using ultrafiltration and reverse osmosis. The major issue arose with the membrane fouling phenomenon, which can reduce the efficiency of separation [12]. Biological treatment with anaerobic digestion is a commonly used process to treat POME due to its low cost and applying thermal or physicochemical treatments [13]. During the anaerobic process, biogas was produced from the open ponding system of the palm oil industry, and the biogas was dissipated or flared into the atmosphere. To improve the sustainability of the palm oil industry, the biogas produced from anaerobic digestion could be captured and utilized as a source of renewable energy [14].

The production of biogas from POME demands recent knowledge in order to enhance the current POME treatment. The simultaneous digestion has been enhanced by the anaerobic digestion by two different metabolic pathways: acetic acid to dismutation into methane (CH_4) and carbon dioxide (CO_2), and hydrogen (H_2) reduction performed by anaerobic methanogenic archaea [15]. However, the process required an enzyme to catalyze the process in CH_4 and CO_2 production, as well as a long reaction time. Ultrasonication was employed to improve the photo fermentative biohydrogen production with a short reaction time (5–60 min) [16]. The H_2 produced by ultrasonication was improved by 50% with the increase in the substrate loading. The use of a Ni-based catalyst can influence the reaction temperature, gas hourly space velocity, support, and promoter to help the conversion of CH_4 to be higher than 70% with an H_2 yield of 45% at more than 700°C [17]. However, the study required a high temperature to obtain the maximum CH_4 conversion. The study by Vijayataghavan et al. [18] demonstrated that aerobic treatment was found to be more efficient than anaerobic treatment, with a COD removal efficiency of 42–83%. However, there is still limited information on how the aerated condition with a short reaction time can strongly influence biogas production from POME.

Dielectric barrier discharge (DBD) has been introduced to optimize the production of biogas from POME, as well as the removal of pollutants [13,19]. DBD was used to reduce the reaction time when producing biogas. With the simple structure and low power consumption, DBD treatment can generate oxidizing radicals (known as active species), such as hydroxyl radicals (•OH), hydrogen peroxide (H_2O_2), and ozone (O_3), from electrical discharges in liquid to increase the chemical kinetic rate. •OH has been proven to have the longest lifetime among the reactive oxygen species, thus allowing it to reduce pollutants in the water and wastewater [20], as well as convert them into biogas. The previous study showed an excellent performance for reducing the organic compounds in POME and increased the conversion of CH_4, H_2, and energy efficiency [13,16,21]. Park et al. [22] applied a DBD reactor to remove the oil mist and enhanced the conversion of oil mist to gas from 6% to 79%. Another result demonstrated that the enhancement of mineralization by DBD treatment can further oxidize intermediates to CO_2 [23]. However, little information is available about the integration treatment for POME for producing biogas. This study introduced DBD treatment combined with the aerated conditions in the production of biogas from POME, as well as the reduction of organic pollutants in terms of COD and BOD. Although Joseph et al. [24] used aeration in DBD treatment to increase the generation of active species and the conversion of biomass, the results are lacking in the discussion of how aeration can alter biogas production. The non-aerated condition (without air supply) was also conducted to compare the performance of DBD treatment for producing biogas and reducing the organic pollutant concentration. In the aerated condition, the presence of dissolved oxygen can assist the oxidation and conversion of organic compounds to CH_4, H_2, and CO_2 [25,26]. This study used the various simulation models and the lab-scale batch DBD with non-aerated and aerated reactors for CH_4, H_2, CO, and CO_2 production. The optimum condition for DBD treatment was applied with an input

voltage of 15, 20, and 25 kV. This study is unique because the integrated system of DBD treatment and the aerated process was performed for the first time, and it demonstrated that the enhancement of biogas production and the reduction of organic pollutants in terms of COD and BOD could be achieved. The study further provides important information to predict the performance of a DBD treatment method in order to attain the optimum amount of CH_4, $H_{2,}$ CO, and CO_2 and the organic pollutant removal from POME on a lab scale.

2. Materials and Methods

2.1. POME

The characteristics of the POME solution used in this study are shown in Table 1 and POME was obtained from a palm oil company located in Indrapura, West Sumatra, Indonesia. The POME was collected from the initial sedimentation tank, and filtration was performed to remove dirt, plant cell debris, fibers, and other solids before the experiment.

Table 1. The characteristics of the POME solution used in this study. Data shown in the tables are mean values from triplicate experimental with standard deviation.

Parameters	Values
pH	8.2 ± 0.67
COD (mg/L)	7210.5 ± 560
BOD (mg/L)	3180.5 ± 241.2
Total solid (TS) (mg/L)	7666.7 ± 1004
DO (mg/L)	1.08 ± 0.07
ORP (mV)	−155 ± 119.6
Temperature (°C)	31.4 ± 0.01

2.2. DBD Treatment under Aerated and Non-Aerated Conditions

The DBD treatment for POME under the non-aerated and aerated conditions is shown in Figure 1. DBD treatment was conducted using a DBD reactor made from glass and had a volume of 3.5 L. The working volume of liquid POME was 800 mL. The system was operated at controlled room temperature (25 °C) and atmosphere pressure (1 atm) following the procedures described previously [13]. The commercial gas sensors TGS series (Figaro, Osaka, Japan) were used to detect the CH_4, H_2, CO, and CO_2. These gas sensors were connected to a data logger Pico 4424 Picoscope (Pico Technology, Eaton Socon, England) and the output data were recorded on a personal computer. The aerated condition was conducted using the Silent β-120 air pump (Nisso, Tokyo, Japan) to supply air at a flow rate of 2.5 L/min.

2.3. Biogas Production Simulation

The study of the biogas production kinetics for the description and evaluation of DBD treatment under non-aerated and aerated conditions was carried out by fitting the experimental data of the biogas production to various model equations. The linear regression of the biogas production in the initial 10 min reaction is expressed by Equation (1). This model is used to explain that biogas production increased linearly with the increase in time.

$$y = a + bt \quad (1)$$

where y is the cumulative biogas production (mL/mg COD), t is the time (min), and a and b are the constants obtained from the intercept and slope of the graph of y vs. t.

The polynomial regression for the initial production of biogas is presented in Equation (2). The model assumes that biogas production follows the multiple linear regression during the reaction, where the increase and decrease in biogas production in the initial 10 min are determined as a 4th-degree polynomial.

$$y = A \times [1 - \exp(-(a_0 + a_1 t + a_2 t^2 + a_3 t^3 + a_4 t^4))] \quad (2)$$

where y is the cumulative biogas production (mL/mg COD) at reaction time t (min), A is the potential maximum biogas yield (mL/mg COD), and a is the constant obtained from the intercept and slope of the graph of y vs. t.

The modified Gompertz model was used to evaluate the performance of the DBD under non-aerated and aerated conditions for biogas production. The cumulative biogas production is described by the following equation:

$$y = A \exp\left\{-\exp\left[\frac{\mu_m e}{A}(\lambda - t) + 1\right]\right\} \quad (3)$$

where y is the cumulative biogas production (mL/mg COD) at reaction time t (min), A is the potential maximum biogas yield (mL/mg COD), μ_m is the maximum biogas production (mL/mg COD/min), λ is a lag phase (min), and e is an Euler's function equal to 2.71983.

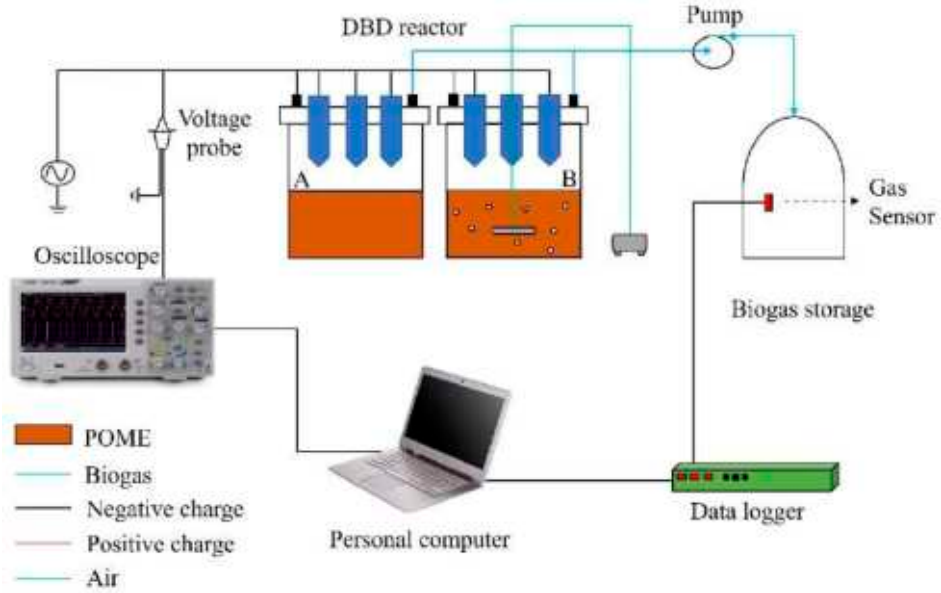

Figure 1. Schematic diagram of the DBD treatment systems. A is the non-aerated condition and B is the aerated condition. Each reactor was supplied with discharge voltages of 15, 20, and 25 kV.

2.4. Organic Pollutant Parameters Characterization

COD and BOD were measured using the procedure described in the APHA standard methods. DO was measured using anHQ40D DO meter (Hach, Tokyo, Japan). pH, ORP, and temperature were measured using the MM-60R multi-water meter (TOA DKK, Tokyo, Japan). A functional group of organic materials observed in the raw POME and after treatment was measured using a C90704 Spectrum IR Version 10.6.1 PerkinElmer, Yokohama, Japan). The samples were measured in a frequency range of 4000–400 cm^{-1} with 1 min scanning and 4 cm^{-1} of the resolution.

2.5. Data Analysis

The significant differences between the mean values of the observed parameters for the treatment of COD and BOD before and after the DBD treatment under non-aerated and aerated conditions were analyzed by two-way analysis of variance (ANOVA) with a 95% confidence level (p = 0.05). The statistical analysis was conducted using the IBM SPSS Statistics (version 24) software program.

3. Results and Discussion

3.1. Cumulative Biogas Volume

Figure 2 shows the cumulative biogas volume produced from POME assisted by DBD treatment under aerated and non-aerated conditions at different discharge voltages. The results show that the cumulative biogas volume increased initially, followed by a decrease

in production rate in all conditions. This implied that some easily biodegradable materials are decomposed at the initial reaction time, leaving the recalcitrant and slow degradable materials. However, the CH_4 profile remained stable until 120 min of reaction at 25 kV. This difference indicates that some parts of substrates were not degraded due to the slower mass transfer [27]. The average cumulative biogas volume produced under non-aerated and aerated conditions is shown in Table 2. It is observed that aerated conditions produced a higher cumulative biogas volume compared with the non-aerated ones. The supplied air under the aerated condition could influence the interaction between active species and organic materials via (1) renewal of atmospheric conditions of the discharge zone; (2) promotion of the diffusion rate of active species; and (3) acceleration of the separation of some violation reaction products, which can renew the atmosphere of the discharge zone and promote the production of active species [28–30]. All of the above mechanisms can enhance the production of biogas from POME using DBD treatment. The finding is concordant with the previous result; assisting the plasma system with an aerated condition increased the conversion of CH_4 and CO_2 by 35% and 28%, respectively, when the voltage reached 80 kV [30]. However, H_2 production under the aerated condition at 25 kV was 6.3 lower in comparison with the non-aerated one. This might be due to a weak reaction between CO_2 and CH_4 under that condition. The air could be the inhibitor and prevent the related reaction to perform between the active species and substrate to form H_2. Overall, the results show that the aerated treatment of POME could enhance CH_4, CO, and CO_2 production by 9.4, 21.5, and 19.6 times more than the non-aerated condition, respectively, at a high discharge voltage, while the highest H_2 production was observed under the aerated condition at 15 kV and was 1.8 higher than the non-aerated condition. The constant supply of dissolved oxygen in the air could maintain the stabilization of organic compounds in POME, resulting in the enhancement of organic compounds' depletion to produce biogas [26]. It is also known that biogas can be produced from biodegradable organic matter [31] in POME, accounting for about 60–65% methane [31]. The previous findings observed a good linear relationship between biogas production and COD removal to assess the treatability of landfill leachate [32]. The aeration condition also help the conversion of organic matter into CO_2, water, and different lower molecular weight organic compounds. Thus, the integrated process of the aerated condition with the high discharge voltage could maintain the existence of active species and the oxidation process to enhance the conversion of organic matter into biogas.

Table 2. The average cumulative biogas volume produced from POME after DBD treatment under aerated and non-aerated conditions at different discharge voltages. The values are shown in mean with standard deviation. The different letters (a–f) indicate that the observed differences are statistically significant at $p < 0.05$.

Conditions	Discharge Voltage (kV)	Cumulative Biogas Volume (mL/mg COD)			
		CH_4	H_2	CO	CO_2
Aerated	15	14.1 ± 6.17^{a}	4.31 ± 1.12^{a}	1.57 ± 0.73^{a}	1.34 ± 0.46^{a}
	20	81.4 ± 12.2^{b}	3.18 ± 1.44^{b}	1.94 ± 0.48^{a}	1.94 ± 0.48^{a}
	25	95.4 ± 8.92^{c}	0.94 ± 0.71^{c}	3.06 ± 0.73^{b}	2.45 ± 0.35^{b}
Non-aerated	15	0.51 ± 0.47^{d}	2.34 ± 0.30^{d}	0.08 ± 0.06^{c}	0.08 ± 0.03^{c}
	20	8.06 ± 1.94^{e}	2.41 ± 0.32^{d}	0.15 ± 0.07^{d}	0.21 ± 0.06^{d}
	25	10.1 ± 1.83^{f}	2.27 ± 0.42^{d}	0.14 ± 0.07^{d}	0.12 ± 0.03^{c}

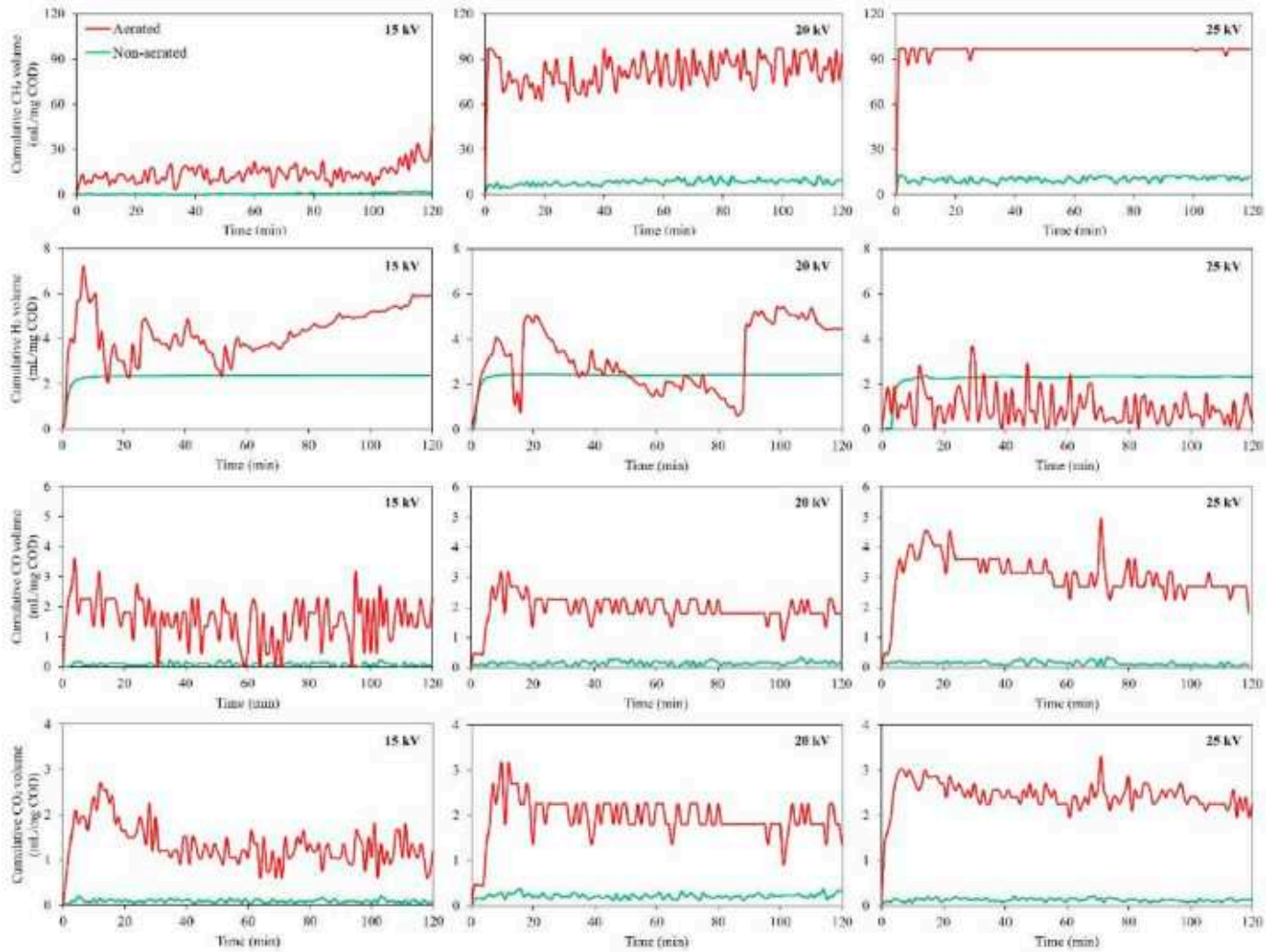

Figure 2. Cumulative biogas volume from POME assisted by DBD treatment under aerated and non-aerated conditions at different discharge voltages of 15, 20, and 25 kV.

In the scenario of discharge voltage, 20 and 25 kV produced more CH_4 compared with that for 15 kV. It is suggested that the higher production of CH_4 reflects the higher content of protein, which is relatively easier to decompose and could be the main substrate responsible for biogas production. This finding is consistent with the result of the functional group parameters by FTIR (see Section 3.4). The peak band of protein materials around 1637 cm^{-1} was sharply observed under all of the conditions. Furthermore, the higher the discharge voltage, the higher the formation rate of active species, such as •O and form C=O and C–H, which will react with the substrate to form CH_4, thus promoting the conversion of CH_4 in the initial time at the discharge voltage of 25 kV [13,33]. The lower discharge voltage was unable to complete the oxidation of the complex organic materials from the plant polymer, thus there was less efficiency for 15 kV in the production of CH_4. These findings are consistent with [13], demonstrating that increasing the discharge voltage to 25 kV could enhance biogas production. However, a slight decline in CO and CO_2 was observed in the aerated condition at 25 kV. The cumulative CO and CO_2 volume declined from the highest volume of 4.49 and 3.30 mL/mg COD to 1.81 and 2.25 mL/mg COD, respectively. The results could lead to the partial dissociation of CO_2 to form CO. A previous study demonstrated that CO_2 dissociation is caused by the highly exciting vibrational states due to high energy in the non-thermal plasma [34]. Thus, promoting a high dissociation of CO_2 to form electronically excited CO. However, this observation was inconsistent with our study, where a high discharge voltage caused the decline of CO and CO_2. Additionally, the

variations in the readings of the produced biogas from experimental data can be attributed to inhibiting gas production, as can be seen in the inconsistency from the graph shown in Figure 2.

3.2. Simulation Models of Biogas Production

The simulation models using linear regression, and polynomial regression were validated using data obtained from the experimental data of biogas production obtained for 10 min of treatment, as shown in Figure 3. In the aerated and non-aerated conditions in the 25 kV scenarios, the simulation result from the modified Gompertz model exhibited an exponential increase in biogas, as shown in Figure 3. A sharp increase in the cumulative biogas was observed under the aerated condition at the input voltage of 25 kV for the simulation data. The presence of oxygen has a significant influence on the production of biogas, resulting in an initial increase in biogas under aerated conditions [28]. The results also indicate that the air supply can accelerate the diffusion of active species and react with the potential substrate to produce biogas, resulting in a high cumulative biogas volume for simulated data, except for H_2. CH_4 production was higher compared with that of H_2, CO, and CO_2 both under non-aerated and aerated conditions. However, both CH_4 and CO_2 increased sharply and reached the maximum rate at the initial time compared with that of H_2 and CO due to the rapid degradation of the substrate caused by the related reaction by the active species. The results further confirm that the higher discharge voltage, despite non-aerated or aerated conditions, forms more active species, such as •O, •OH, and ozone in the water. A higher voltage resulted in more energy absorbed by C=O in CO_2 before breaking down, thus increasing CO [33]. Based on the experimental data observation, CH_4 increased sharply before 10 min and reach its maximum cumulative volume higher than CO_2. However, both the experimental data and simulated data confirm that CO_2 was produced in a lower state compared with that for CH_4. This is contradicted by the fact that enhancing the discharge voltage will increase the electron density and concentration of the active species, which energize and activate CH_4 and CO_2 particles resulting in a similar increase in CH_4 and CO_2 [33].

By comparing the simulation data to the data obtained from the experimental data, the model simulation showed the biogas production rate rising exponentially with treatment time, and becoming stable after reaching the maximum points. The inconsistency trends from the experimental data revealed that the POME contained a variety of organic materials that could influence the production rate during DBD treatment. This suggested that the reaction between active species produced from electric discharge was only performed on the surface of the reactor, thus only some parts of organic compounds were converted into biogas [13]. Figure 3a,b shows the comparison results between the three models: linear regression, polynomial regression, and the modified Gompertz model. Linear regression was well fitted on the experimental data for only the initial production time of CO and CO_2 under the aerated condition (Table 3). The R^2 value of CO of 0.906 and CO_2 of 0.835 showed that linear regression is a good model for use when explaining the initial production of biogas using DBD treatment under the aerated condition. For polynomial regression, the initial increase and decrease in cumulative biogas volume could be estimated and its correlation coefficient for biogas under the aerated and non-aerated conditions at 25 kV are presented in Table 3. The high R^2 for biogas under both the aerated and non-aerated conditions suggests that the polynomial regression model has the potential to predict the cumulative biogas production, and their correlation between the experimental data and the model is at an acceptable level for the initial production time. The modified Gompertz model was used to fit the data from the DBD treatment and built a higher R^2 only for CH_4 under the aerated condition, H_2 under the non-aerated condition, and somehow CO_2 under the aerated condition, as shown in Figure 3 and Table 3. This suggests that the modified Gompertz model has the potential to predict cumulative biogas volume for the entire reaction time.

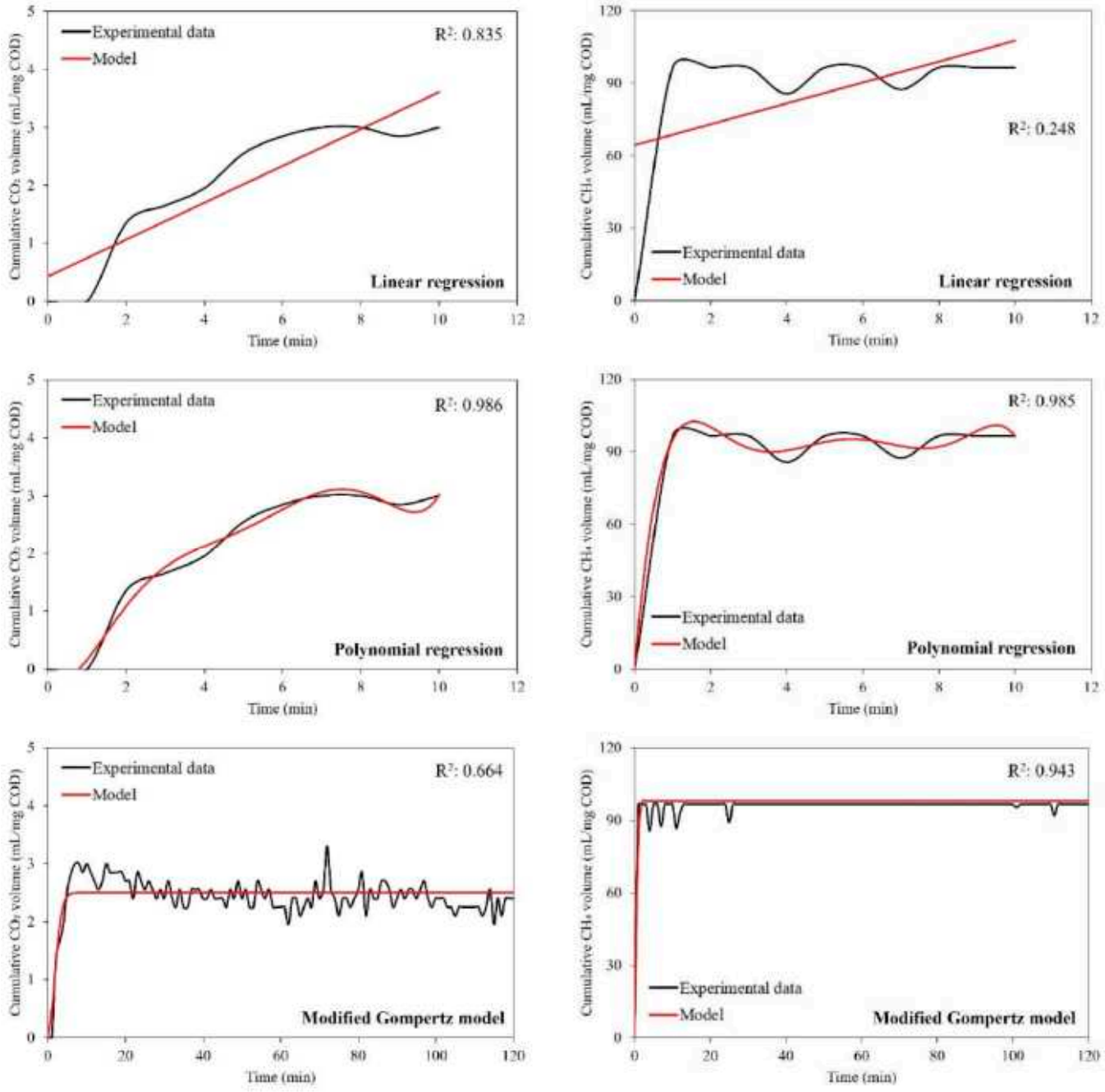

Figure 3. Simulated and experimental data of cumulative biogas volume of (**a**) CO_2 and (**b**) CH_4 from POME assisted by DBD treatment under the aerated conditions at a discharge voltage of 25 kV.

However, the purposed models do not fit well with all the biogas profiles under all of the conditions. Only the initial biogas production time fitted well with the polynomial regression and somehow linear regression.Thus, the models cannot explain the correlation between the experimental data and the models for the entire reaction time. Taking account into this, the modified Gompertz model merely fitted on CH_4, H_2, and CO_2. However, the model cannot be applied to other biogas under different conditions. This might be due to the error consisting of the replicate measurement for the biogas analysis. Therefore, new models will be addressed to validate the obtained experimental data by DBD treatment.

Table 3. Comparison of results between experimental data and Gompertz model for experimental dan simulated data observed non-aerated conditions at 25 kV.

Condition	Models	Parameters	CH_4	H_2	CO	CO_2
Non-aerated	Linear regression	a	0.263	0.191	0.012	0.009
		R^2	0.064	0.748	0.367	0.416
	Polynomial regression	a_0	−0.095	0.082	0.002	0.003
		a_1	25.92	−0.661	0.363	−0.016
		a_2	18.23	0.427	−0.299	0.051
		a_3	5.696	−0.054	0.109	−0.021
		a_4	0.899	0.001	−0.019	0.004
		R^2	0.922	0.963	0.889	0.884
	Modified Gompertz model	A (mL/mg COD)	11.65	2.359	0.12	0.116
		μ_m (mL/mg COD)	12.14	2.935	0.339	0.207
		λ (min)	2.315	2.126	5.652	4.726
		R^2	0.253	0.955	0.037	0.191
Aerated	Linear regression	a	4.325	0.005	0.454	0.318
		R^2	0.248	0.001	0.906	0.835
	Polynomial regression	a_0	0.258	0.026	0.007	−0.032
		a_1	186.3	1.393	2.137	−0.902
		a_2	−123.9	−0.319	−2.651	1.639
		a_3	38.02	−0.018	1.247	−0.658
		a_4	−5.915	0.001	−0.247	0.121
		R^2	0.985	0.568	0.996	0.986
	Modified Gompertz model	A (mL/mg COD)	94.31	0.985	2.675	2.574
		μ_m (mL/mg COD)	96.59	3.627	4.949	3.301
		λ (min)	3.512	3.251	2.458	2.354
		R^2	0.943	0.013	0.464	0.664

3.3. Changes in COD and BOD

The changes in COD and BOD after DBD treatment under aerated and non-aerated conditions at different discharge voltages and their removal are shown in Figure 4 and Table 4, respectively. After 120 min of treatment, the COD dropped from 7210 mg/L in raw POME to below 500 mg/L after DBD treatment in all of the operating conditions, except at the discharge voltage of 25 kV. Compared with the non-aerated conditions, aerated conditions at different discharge voltages caused a significant drop ($p < 0.05$) of COD, especially at the input voltage of 20 kV. The increase in input voltage for DBD treatment to 20 kV caused a high removal rate for COD and BOD. Increasing the discharge voltage, the density and the energy of electrons increase and result in the increased formation of active species, such as ozone, •O, and •OH [35–37]. The degradation of BOD followed similar trends to COD, where aerated conditions decreased more BOD compared with the non-aerated ones. COD and BOD removal improved greatly when the aerated condition was performed and the final COD and BOD values were below 200 mg/L and 100 mg/L, respectively, in all of the different discharge voltages. Overall, the removal of COD and BOD for aerated and non-aerated conditions was above 90%, which demonstrates a good treatment performance for the DBD (Table 4).

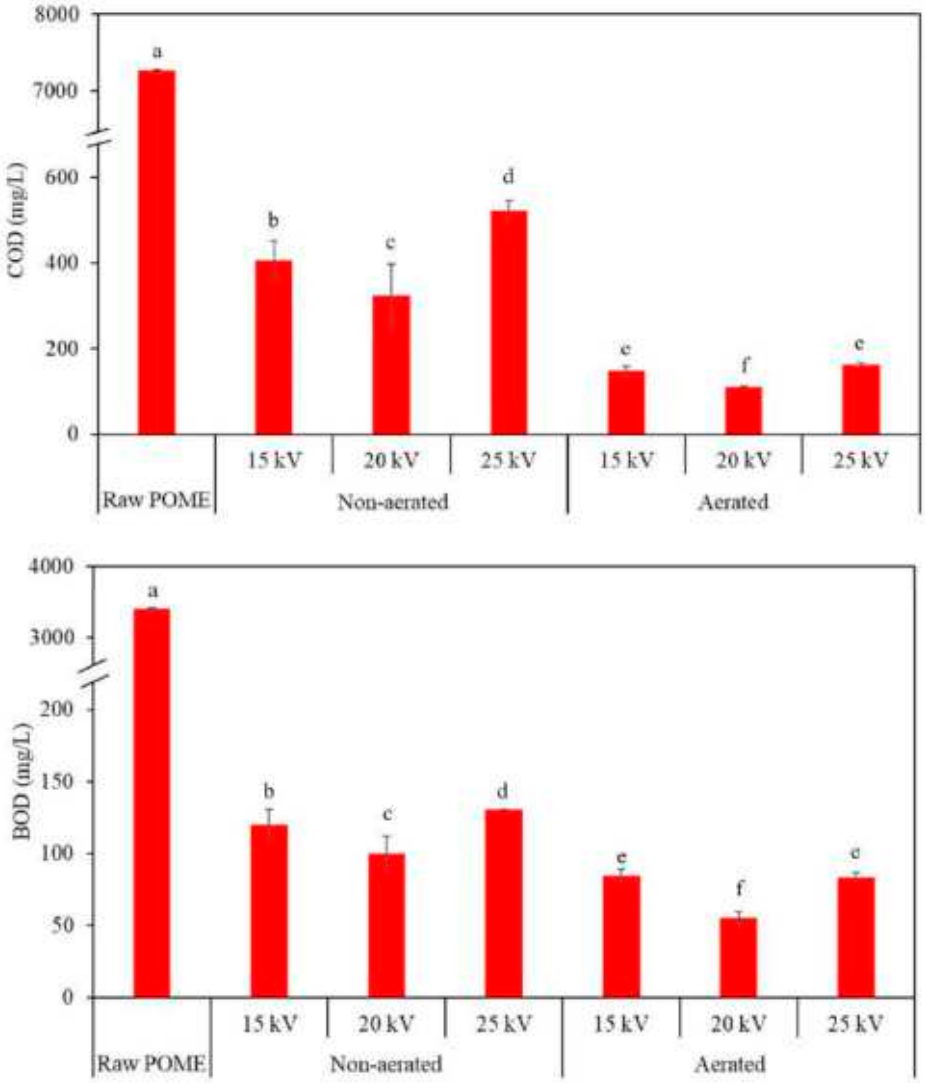

Figure 4. Changes in COD and BOD after DBD treatment under aerated and non-aerated conditions at different discharge voltages of 15, 20, and 25 kV. The different letters (a–f) indicate that the observed differences are statistically significant at $p < 0.05$.

Table 4. The removal percentage of COD and BOD in DBD treatment under aerated and non-aerated conditions at different discharge voltages. The values are shown in mean with standard deviation.

Conditions	Discharge Voltage (kV)	Removal Percentage (%)	
		COD	BOD
Aerated	15	97.9 ± 0.15	97.3 ± 0.14
	20	98.5 ± 0.02	98.3 ± 0.15
	25	97.7 ± 0.04	97.4 ± 0.08
Non-aerated	15	94.4 ± 0.64	96.2 ± 0.33
	20	95.5 ± 1.02	96.8 ± 0.39
	25	92.7 ± 0.31	95.9 ± 0.01

There were significant differences in COD and BOD removal in all different input voltages under aerated and non-aerated conditions that influence biogas production. The higher the discharge voltage, the more energy is consumed by chemical processes such as oxidation. Aerated condition supplied air and partial volatilization might occur during treatment due to the bubble aeration effect. In this study, some organic materials might volatilize during aerated conditions and the presence of electric discharge increased the removal of COD and BOD. The supplied air could also promote the diffusion of active

species, which will increase the probability of contact between active species and organic materials [38]. Therefore, aerated conditions with an increase in discharge voltage were meaningful for the removal of COD and BOD. However, the aerated condition at 25 kV resulted in a high residual COD and BOD and a lower removal percentage compared with that of 20 kV. This might be because of air bubbling that can shorten the reaction of active species and organic materials, thus decreasing the utilization efficiency of active species [36,38]. Moreover, the high residual COD and BOD after DBD treatment both under non-aerated and aerated at 25 kV demonstrated that only some active species reacted with the organic materials due to the poor distribution inside the reactors. These findings are concordant with the previous study, where air greatly influenced the removal of organic materials in terms of TOC due to the promotion of the production of active species [38].

From Figure 2, it can be understood that the aerated conditions with a high discharge voltage produced the maximum biogas yield compared with the non-aerated one. It is also observed that the amount of biogas produced increased with the increase in the removal percentage of organic materials in terms of COD and BOD. The abundant biodegradable organic substrate in POME can be easily degraded by oxidation due to the bubbling and the formation of active species from DBD at a high discharge voltage. The lower biogas produced under non-aerated conditions might be due to poor biodegradation of the organic substrates.

3.4. Functional Group Characteristics of POME before and after Treatment by FTIR

Figure 5 and Table 5 show the presence of functional groups in POME before and after treatment. The band of 3300–3400 cm^{-1} was assigned to the O-H stretching in the carboxyl groups, which is believed to be the appearance of cellulose compounds [39]. The band did not change significantly after DBD treatment, which implied the corresponding treatment conditions were poor for initiating the depolymerization of macromolecular in terms of hydrogen bond loss. The peak at 2104 cm^{-1} in raw POME was associated with the conjugated cyclic compounds, which may be aromatic or nonaromatic [40]. The band at 1637 cm^{-1} was attributed to the C=O and C-N stretching from proteins and was observed in both raw POME and after treatments. There was no significant change in the protein band in raw POME and after treatments, suggesting that the proteins had not been damaged by the DBD treatment. The weak shoulder in 1012 cm^{-1} was attributed to the C-O in the alkoxy groups of polysaccharides [41]. The peak vanished after DBD treatment under both aerated and non-aerated conditions, demonstrating the decomposition of polysaccharides by active species from DBD treatment. The decomposition of polysaccharides might cause the cleaving of the CH vibration due to the reaction of active species and cellulose structure [42,43]. The peak band between 500–700 cm^{-1} was assigned to silica impurities and clay minerals that might be in a complex with humic acids [44].

Table 5. FTIR frequency ranges and functional groups in raw POME and POME after DBD treatment under non-aerated and aerated conditions.

Peak Wavenumbers (cm^{-1})	FTIR Band	Possible Functional Groups or Compounds	References
3300–3400	O-H stretching	Hydroxyl and carboxyl groups	[45]
2920–2926	C-H asymmetric	Aliphatic methylene	[46]
2850–2852	C-H symmetric	Aliphatic methylene	[46]
2100–2500	C=C conjugated		
1720–1740	C=O stretching	Aldehyde, ketone, carboxylic acids, esters (lipids)	[45]
1620–1670	C=O stretching C-N stretching	Amides I (protein)	[45]
1546	N-H in plane	Amides II	[45]
1040–1080	C-O-C stretching C-O stretching	Polysaccharides Lignin	[47]

Table 5. *Cont.*

Peak Wavenumbers (cm^{-1})	FTIR Band	Possible Functional Groups or Compounds	References
872–875	C-O out of plane	Carbonate	[47]
500–730	S-S stretching C-S stretching	Disulfides Thioethers	[47]
430–500	S-S stretching	Polysulfides	[47]

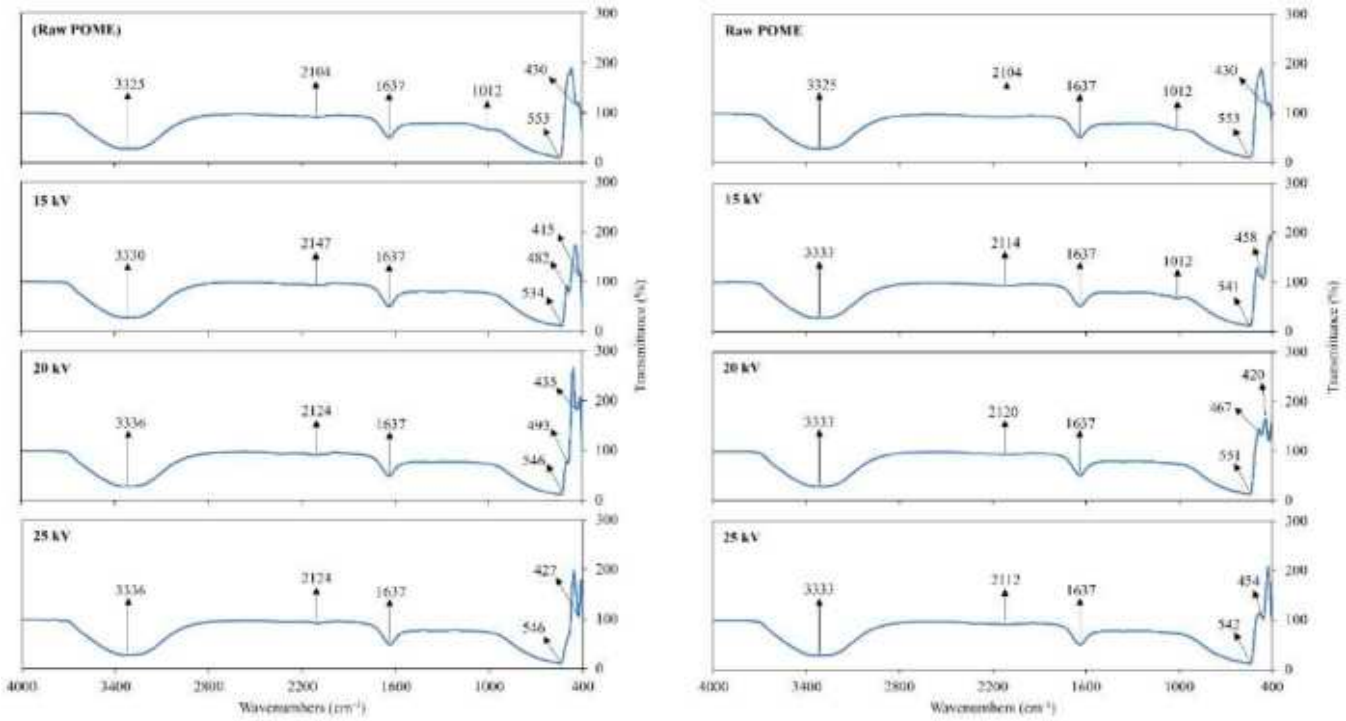

(**a**) (**b**)

Figure 5. FTIR spectra of raw POME and POME after DBD treatment under (a) aerated and (b) non-aerated conditions at different discharge voltages of 15, 20, and 25 kV.

4. Conclusions

This study investigated the biogas production from POME using DBD treatment under aerated and non-aerated conditions at different discharge voltages of 15, 20, and 25 kV. The maximum cumulative biogas volume produced from POME in the order of CH_4, H_2, CO, and CO_2 was 95.4 ± 8.89, 0.94 ± 0.71, 3.06 ± 0.73, and 2.45 ± 0.35 mL/mg COD from the aerated condition, and 10.1 ± 1.83, 2.27 ± 0.42, 0.14 ± 0.07, and 0.12 ± 0.03 mL/mg COD from the non-aerated condition at 25 kV, respectively. The results further confirmed that the DBD treatment with a high discharge voltage assisted with the aerated condition and produced higher biogas compared with the non-aerated one. The aeration could enhance the diffusion of the produced active species in the POME solution, thus increasing the performance of the DBD treatment. The data obtained from the experimental data were validated using linear regression, polynomial regression, and the modified Gompertz model, and show the differences between that obtained from the experiment and that generated from the simulation model. The reason for this could be the deterrent factors that occurred in the laboratory experiment and led to the low or unstable biogas production. Only polynomial regression predicted the initial biogas production well. The changes in organic pollutants in terms of COD and BOD were significantly observed when POME was treated under aerated and non-aerated conditions. The high removal rate of COD and BOD (>95%) supported the findings that DBD treatment under aerated conditions, especially at

a high discharge voltage, converted the organic materials into biogas. The changes in the band peak of organic materials assessed by FTIR explained the changes in polysaccharides and protein materials as they reacted with active species to form biogas (the vanished peak of 1012 cm^{-1} after aerated and non-aerated conditions). The discharge voltages and aerated conditions had a great impact on the production of biogas and the reduction of organic pollutants. This indicates that active species generated from the DBD treatment played critical roles in the organic material transformations as the system was assisted by air from the system. The significant differences in aerated and non-aerated conditions from DBD treatment further require special attention for future applications in order to produce biogas, as well as for the reduction of organic pollutants from wastewater in general.

Author Contributions: Conceptualization, R.D., M.Y.R. and A.H.; methodology, R.D., A.H., N.N., M.M.R. and J.A.F.; software, N.N. and M.M.R.; validation, R.D., M.Y.R. and A.H.; formal analysis, N.N. and M.M.R.; investigation, R.D. and N.N.; data curation, M.Y.R. and M.M.R.; writing—original draft preparation, M.Y.R. and R.D; writing—review and editing, M.Y.R., R.D. and A.H.; supervision, R.D., A.H. and J.A.F.; funding acquisition, R.D. All authors have read and agreed to the published version of the manuscript.

Funding: This research was supported by the Ministry of Education, Culture, Research, and Technology of Indonesia with grant number 067/LPPM/Hatta-P/VI-2022.

Data Availability Statement: Not applicable.

Acknowledgments: We would like to thank the Water and Wastewater Laboratory team of the Department of Chemical Engineering for the investigation and file survey.

Conflicts of Interest: The authors declare no conflict of interest. The funders had no role in the design of the study; in the collection, analyses, or interpretation of data; in the writing of the manuscript; or in the decision to publish the results.

References

1. The Recent Development of the Indonesian Palm Oil Industry. Available online: https://gapki.id/en/news/18397/the-recent-development-of-the-indonesian-palm-oil-industry (accessed on 24 August 2022).
2. Palm Oil Industry in Indonesia—Statistics & Facts. Available online: https://www.statista.com/topics/5921/palm-oil-industry-in-indonesia/#topicHeader__wrapper (accessed on 24 August 2022).
3. Sani, K.; Kongjan, P.; Pakhathirathien, C.; Cheirslip, B.; O-Thong, S.; Raketh, M.; Kana, R.; Jariyaboon, R. Effectiveness of using two-stage anarobic digestion to recover bio-energy from high strength palm oil mill effluents with simultaneous treatment. *J. Water Process Eng.* **2021**, *39*, 101661. [CrossRef]
4. Tanikkul, P.; Boonyawanich, S.; Pisutpaisal, N. Production of methane from ozonated palm oil mill effluent. *Int. J. Hydrog. Energy* **2019**, *44*, 29561–29567. [CrossRef]
5. Leano, E.P.; Anceno, A.J.; Babel, S. Ultrasonic pretreatment of palm oil mill effluent: Impact on biohydrogen generation, and underlying microbial communities. *Int. J. Hydrog. Energy* **2017**, *37*, 12241–12249. [CrossRef]
6. Kamal, S.A.; Jahim, J.M.; Anuar, N.; Hassan, O.; Daud, W.R.W.; Manor, M.F.; Rashid, S.H. Pre-treatment effect of palm oil mill effluent (POME) during hydrogen production by a local isolate *Clostridium butyricum*. *Int. J. Adv. Sci. Eng. Inf. Technol.* **2014**, *2*, 325–331. [CrossRef]
7. Nasrullah, M.; Singh, L.; Mohamad, S.; Norsita, S.; Krishnan, S.; Wahida, S.; Zularisman, A.W. Treatment of palm oil mill effluent by electrocoagulation with presence of hydroxide peroxide as oxidizing agent and polialuminum chloride as coagulant-aid. *Water Resour. Indust.* **2017**, *17*, 7–10. [CrossRef]
8. Saad, M.S.; Joe, N.C.; Shuib, H.A.; Wirzal, M.D.H.; Putra, Z.A.; Khan, M.R.; Busquets, R. Techno-economic analysis of an integrated electrocoagulation-membrane system in treatment of palm oil mill effluent. *J. King Saud Univ. Sci.* **2022**, *34*, 102015. [CrossRef]
9. Bashir, M.J.; Han, T.M.; Wei, L.J.; Aun, N.C.; Amr, S.S.A. Polishing of treated palm oil mill effluent (POME) from ponding system by electrocoagulation process. *Water Sci. Technol.* **2016**, *73*, 2704–2712. [CrossRef]
10. Halim, N.S.A.; Wirzal, M.D.J.; Bilad, M.R.; Nordin, N.A.H.M.; Putra, Z.A.; Sambudi, N.S.; Yusoff, A.R.M. Improving performance of electrospun nylon 6,6 nanofiber membrane of produced water filtration via solvent vapor treatment. *Polymers* **2019**, *11*, 2117. [CrossRef]
11. Zhang, M.; Yao, L.; Maleki, E.; Liao, B.-Q.; Lin, H. Membrane technology for microalgal cultivation and dewatering: Recent progress and challenges. *Algal Res.* **2019**, *44*, 101686. [CrossRef]

12. Elma, M.; Rahma, A.; Pratiwi, A.E.; Rampun, E.L.A. Coagulation as pretreatment for membrane-based wetland saline water desalination. Coagulation as pretreatment for membrane-based wetland saline water desalination. *Asia-Pac. J. Chem. Eng.* **2020**, *15*, e2461. [CrossRef]
13. Desmiarti, R.; Rosadi, M.Y.; Emeraldi, P.; Hazmi, A. Integrated evaluation of POME treatment by dielectric barrier discharge based on yield of H_2 and CH_4, EEM and removal of COD. *J. Chem. Eng. Japan* **2021**, *54*, 255–259. [CrossRef]
14. Liew, Z.K.; Chan, Y.J.; Ho, Z.T.; Yip, Y.H.; Teng, M.C.; Ameer Abbas bin, A.I.T.; Chong, S.; Show, P.L.; Chew, C.L. Biogas production enhancement by co-digestion of empty fruit bunch (EFB) with palm oil mill effluent (POME): Performance and kinetic evaluation. *Renew. Energy* **2021**, *178*, 766–777. [CrossRef]
15. Wadchasit, P.; Suksong, W.; O-Thong, S.; Nuithitikul, K. Development of a novel reactor for simultaneous production of biogas from oil-palm empty fruit bunches (EFB) and palm oil mill effluents (POME). *J. Environ. Chem. Eng.* **2021**, *9*, 105209. [CrossRef]
16. Budiman, P.T.; Wu, T.Y. Ultrasonication pre-treatment of combined effluents from palm oil, pulp and paper mills for improving photofermentative biohydrogen production. *Energy Convers. Manag.* **2016**, *119*, 142–150. [CrossRef]
17. Pham, C.Q.; Siang, T.J.; Kumar, P.S.; Ahmad, Z.; Xiao, L.; Bahari, M.B.; Cao, A.N.T.; Rajamoham, N.; Qazaq, A.S.; Kumar, A.; et al. Production of hydrogen and value-added carbon materials by catalytic methane decomposition: A review. *Environ. Chem. Lett.* **2022**, *20*, 2339–2359. [CrossRef]
18. Vijayataghavan, K.; Ahmad, D.; bin Abdul Aziz, M.E. Aerobic treatment of palm oil mill effluent. *J. Environ. Manag.* **2007**, *82*, 24–31. [CrossRef]
19. Hazmi, A.; Desmiarti, R.; Emeraldi, P.; Hamid, M.I.; Edwardo, E.; Waldi, E.P. Preliminary study on biogas production from POME by DBD plasma. *Telkomnika* **2017**, *15*, 554–559. [CrossRef]
20. Attri, P.; Kim, Y.H.; Park, D.H.; Park, J.H.; Hong, Y.J.; Uhm, H.S.; Kim, K.N.; Fridman, A.; Choi, E.H. Generation mechanism of hydroxyl radical species and its lifetime prediction during the plasma initiated ultraviolet (UV) photolysis. *Sci. Rep.* **2015**, *5*, 9332. [CrossRef]
21. Zeng, X.Y.; Wang, L.; Wu, C.F.; Wang, J.Q.; Shen, B.X.; Tu, X. Low temperature reforming of biogas over K-, Mg-, and Ce-promoted Ni/Al_2O_3 catalysts for the production of hydrogen rich syngas: Understating the plasma-catalytic synergy. *Appl. Catal. B* **2018**, *224*, 469–478. [CrossRef]
22. Park, S.S.; Kang, M.S.; Hwang, J. Oil mist collection and oil mist-to-gas conversion via dielectric barrier discharge at atmospheric pressure. *Separ. Purif. Technol.* **2015**, *151*, 324–331. [CrossRef]
23. Li, J.; Zheng, Z.; Cui, X.; Liu, Y.; Fan, T.; Liu, Y.; Chang, D.; Yang, D. Decomposition of naphthalene by dielectric barrier discharge in conjunction with a catalyst at atmospheric pressure. *Catalysts* **2022**, *12*, 740. [CrossRef]
24. Joseph, C.G.; Farm, Y.Y.; Taufiq-Yap, Y.H.; Pang, C.K.; Nga, J.L.H.; Puma, G.L. Ozonation treatment processes for the remediation of detergent wastewater: A comprehensive review. *J. Environ. Chem. Eng.* **2021**, *9*, 106099. [CrossRef]
25. Lok, X.; Chan, Y.J.; Foo, D.C.Y. Simulation and optimisation of full-scale palm oil mill effluent (POME) treatment plant with biogas production. *J. Water Process Eng.* **2020**, *38*, 101558. [CrossRef]
26. Shammas, N.; Wang, L. *Biosolids Treatment Process*; Humana Press: Totowa, NJ, USA, 2022; pp. 177–205.
27. Guo, P.; Zhou, J.; Ma, R.; Yu, N.; Yuan, Y. Biogas production and hat transfer performance of multiphase flow digester. *Energies* **2019**, *12*, 1960. [CrossRef]
28. Aggelopoulos, C.A.; Gkelios, A.; Klapa, M.I.; Kaltsonoudis, C.; Svarnas, P.; Tsakiroglou, C.D. Parametric analysis of the operation of a non-thermal plasma reactor for the remediation of NAPL-polluted soils. *Chem. Eng. J.* **2016**, *301*, 353–361. [CrossRef]
29. Li, X.; Zhang, H.; Luo, Y.; Teng, Y. Remediation of soil heavily polluted with polychlorinated biphenyls using a low-temperature plasma technique. *Fron. Environ. Sci. Eng.* **2013**, *8*, 277–283. [CrossRef]
30. Mao, M.; Tan, Z.; Zhang, L.; Huang, Q. Plasma-assisted biogas reforming to syngas at room temperature condition. *J. Energy Inst.* **2018**, *91*, 172–183. [CrossRef]
31. Zhang, C.; Wang, A.; Jia, J.; Zhao, L.; Song, W. Effect of parameters on anaerobic digestion EGSB reactor for producing biogas. *Procedia Eng.* **2017**, *205*, 3749–3754. [CrossRef]
32. Gülşen, H.; Turan, M. Anaerobic treatability of sanitary landfill leachate in a fluidized bed reactor. *Turk. J. Eng. Env. Sci.* **2004**, *28*, 297–305.
33. Zhu, F.; Zhang, H.; Yan, X.; Yan, J.; Ni, M.; Li, X.; Tu, X. Plasma-catalytic reforming of CO_2-rich biogas over Ni/γ-Al_2O_3 catalysts in a rotating gliding arc reactor. *Fuel* **2017**, *199*, 430–437. [CrossRef]
34. Tang, Q.; Jiang, W.; Cheng, Y.; Ling, S.; Lim, T.M.; Xiong, J. Generation of reactive species by gas-phase dielectric barrier discharge. *Ind. Eng. Chem. Res.* **2011**, *50*, 9839–9846. [CrossRef]
35. Geng, C.; Wu, C.; Wang, H.; Yi, C. Effect of chemical parameters on pyrene degradation in soil in a pulsed discharge plasma system. *J. Electrost.* **2015**, *73*, 38–42. [CrossRef]
36. Wang, X.; Gong, Y.; Qin, J.; Cheng, J.; Gong, C.; Jiang, D. Deep removal of organic matter in glyphosate contained industrial waste salt by dielectric barrier discharge plasma. *J. Environ. Chem. Eng.* **2021**, *9*, 106295. [CrossRef]
37. Desmiarti, R.; Hazmi, A.; Trianda, Y.; Sari, E. Removal of pathogenic bacteria from water by radio-frequency thermal plasma treatment. *Res. J. Pharm. Biol. Chem. Sci.* **2015**, *6*, 889–897.
38. Abdulla, H.A.; Minor, E.C.; Dias, R.F.; Hatcher, P.G. Changes in the compounds classes of dissolved organic matter along an estuarine transect: A study using FTIR and 13C NMR. *Geochim. Cosmochim. Acta* **2010**, *74*, 3815–3838. [CrossRef]

39. Baharuddin, A.S.; Rahman, N.A.A.; Shah, U.K.M.; Hassan, M.A.; Wakisaka, M.; Shirai, Y. Evaluation of pressed shredded empty fruit bunch (EFB)-palm oil mill effluent (POME) anaerobic sludge based compost using Fourier transform infrared (FTIR) and nuclear magnetic resonance (NMR) analysis. *Afr. J. Biotechnol.* **2011**, *10*, 8082–8089.
40. Muhidinov, Z.K.; Boboklonov, J.T.; Ismoilov, I.B.; Strahan, G.D.; Chau, H.K.; Hotchkiss, A.T.; Liu, L.S. Characterization of two types of polysaccharides from *Eremurus hissaricus* roots growing in Tajikistan. *Food Hydrocoll.* **2020**, *105*, 105768. [CrossRef]
41. O'Connor, R.T.; DuPré, E.F.; McCall, E.R. Applications of infrared absorption spectroscopy to investigations of cotton and modified cottons: Part 1: Physical and crystalline modifications and oxidation. *Text. Res. J.* **1958**, *28*, 382–392. [CrossRef]
42. Wright, A.; Rollinson, A.; Yadav, D.; Liswoki, S.; Iza, F.; Holdich, R.; Radu, T.; Bandulasena, H.C.H. Plasma-assisted pre-treatment of lignocellulosic biomass for anaerobic digestion. *Food Bioprod. Process* **2020**, *124*, 287–295. [CrossRef]
43. Lei, Y.; Sung, D.; Dang, Y.; Chen, H.; Zaho, Z.; Zhang, Y.; Holmes, D.E. Stimulation of methanogenesis in anaeerobic digesters treating leachate from a municipal solid waste incineration plant with carbon cloth. *Bioresour. Technol.* **2016**, *222*, 270–276. [CrossRef]
44. Rago, L.; Zecchin, S.; Marzorati, S.; Goglio, A.; Cavalca, L.; Christiani, P.; Schievano, A. A study of microbial communities on terracotta separator and on biochatode of air breathing microbial fuel cells. *Bioelectrochemistry* **2018**, *120*, 18–26. [CrossRef] [PubMed]
45. Chevali, V.; Kandare, E. *Biopolymers and Biotech Admixtures for Eco-Efficient Construction Materials*; Elsevier Academic Press: Cambridge, MA, USA, 2016; pp. 275–304.
46. Provenzano, M.R.; Malerba, A.D.; Pezzolla, D.; Gigliotti, G. Chemical and spectroscopic characterization of organic matter during the anaerobic digestion and successive composting of pig slurry. *Waste Manag.* **2014**, *34*, 653–660. [CrossRef] [PubMed]
47. Jones, J.R.; Hench, L.L. *Encyclopedia of Condensed Matter Physics*; Elsevier Academic Press: Cambridge, MA, USA, 2005; pp. 108–116.